Fault Tolerant Key Generation and Secure Spread Spectrum Communication

Arslan Javaid Majid, Hussein Moradi, and Behrouz Farhang-Boroujeny, *Senior Member, IEEE*

***Abstract*— A fundamental characteristic of wireless communications is in its broadcast nature, which allows accessibility of information without placing restrictions on a user's location. However, accessibility also makes wireless communications vulnerable to eavesdropping. In this context, this paper presents a two-part secure information transmission system. The first part makes use of reciprocity in wireless channels to allow for two asynchronous transceivers to obtain a pair of similar keys. Moreover, a unique augmentation, called strongest path cancellation (SPC), is applied to the keys. In the second part, the concept of artificial noise is introduced to the spread spectrum systems. Keys generated in the first part are used in the spread spectrum system and artificial noise is added to enhance the security of the communications. Two attacks on the proposed security solution are evaluated. First, an adversary following the same steps as the legitimate users is considered. Here, simulation and experimentation results show that SPC provides a boost to security against this type of adversary. The second attack studies an adversary with significant blind detection capabilities. Our observations on this attack indicate that when an ample amount of artificial noise can be used, two legitimate parties can communicate multiple information symbols per key.**

***Index Terms*— Reciprocal channel key exchange, physical layer security, spread-spectrum, secure information transmission.**

I. Introduction

WE CONSIDER the security issues involved in spread-spectrum (SS) wireless communication systems. Such systems are used in applications which require resilience to harsh environments, resistance to channel fading through frequency diversity, low probability of detection (LPD), and low probability of interception (LPI) [1]. However, as with any wireless communication system, due to the broadcast nature of the communication, a passive eavesdropper (Eve) within range of broadcast can obtain the transmitted signal between a pair of legitimate users (Alice and Bob). Given a sufficient number of signal samples, the adversary may be able to identify the spreading sequence and, hence, recover the transmitted information.

Manuscript received November 1, 2016; revised March 21, 2017; accepted May 17, 2017. Date of publication June 9, 2017; date of current version August 10, 2017. This work was supported by Battelle Energy Alliance, LLC with the U.S. Department of Energy under Contract DE-AC07-05ID14517. The associate editor coordinating the review of this paper and approving it for publication was J. Lee. *(Corresponding author: Arslan Javaid Majid.)*

A. J. Majid and B. Farhang-Boroujeny are with The University of Utah, Salt Lake City, UT 84112 USA (e-mail: arslan.majid@utah.edu; farhang@ece.utah.edu).

H. Moradi is with The Idaho National Laboratory, Idaho Falls, ID 83402 USA (e-mail: hussein.moradi@inl.gov).

Color versions of one or more of the figures in this paper are available online at http://ieeexplore.ieee.org.

Digital Object Identifier 10.1109/TWC.2017.2711617

As of today, the security in SS is limited by their spreading sequences. Often, it is assumed that a SS message signal transmitted by Alice cannot be recovered without the right spreading code. However, very little has been said on true security of the SS systems and most security solutions in the implementations of SS are limited. In fact, surveys in [2] and [3] confirms that research in this area is open.

Real-world implementations of SS systems, e.g., IS-95 and IS-2000 standards [4], have used long, periodic psuedo-noise (PN) sequences in combination with a mask for physical-layer security. The mask is shared between the mobile and base station, while the long-code PN sequence is defined by a 42-bit linear feedback shift register with a *publicly* known characteristic polynomial. Despite the long period of the PN sequence, it has been shown that an adversary with reasonable computational resources can implement a brute force attack in as little as 2.2 seconds [2]. Li *et al.* [5] showed that an adversary with knowledge of the characteristic polynomial need only intercept 42 continuous long-code PN sequence bits to regenerate the entire long-code sequence. A solution proposed in [5] uses a combination of cryptography and physical-layer techniques to aid in scrambling the long PN sequence. However, the security of this method is reliant on the assumption of a computationally bounded adversary and is limited by secrecy of the encryption session key, assumed to be known *a-priori* in [5] between Alice and Bob.

Cryptography based solutions require key establishment, and key establishment for wireless networks is generally handled through public key cryptography (PKC) [6]. PKC is comprised of a set of protocols including the well-known Diffie-Hellman [7]. Here, session keys are generated with the help of *trapdoor one-way functions* - functions that are computationally difficult to compute without a special code, the code being provided to the legitimate users by the certificate authority. PKC-based methods require a lower bound assumption on the computational power of the adversary and are mathematically unproven to be secure [8]. Additionally, they are computationally expensive, hindering its application in devices with limited battery power.

An interesting alternative to the cryptography-based approach to increase physical-layer security for Alice and Bob is to make use of the following properties of the wireless channel:

- *Channel reciprocity*: The wireless channel between any pair of transceivers using the same wireless link experience the same fading properties (gains, phase shifts, and multipath delays).

- *Channel randomness*: Channel fading across time and frequency benefits from randomness due to Doppler spread and multipath delay spread, respectively.
- *Channel independence over space*: An adversary located more than a few wavelengths away from the legitimate users experiences a different random and uncorrelated channel.

These properties of the wireless channel allow for a pair of users to effectively share a secret - the secret being a realization of the channel - which is statistically uncorrelated for a third party spatially separated from the legitimate users.

Application of wireless channels in physical-layer security is not new, and many papers have considered this topic. A good set of surveys for this area are [8]–[12]. Three prominent research areas in this line of work are: 1) physical-layer key generation, 2) secure information transmission, and 3) theoretical bounds of secret key and secrecy capacity.

In physical-layer key generation, the wireless channel is used to obtain a secret key. In general, the procedure to generate a key from the fading channel requires the following steps: 1) randomness sharing, 2) information reconciliation, 3) privacy amplification, and 4) secure communication [13]. In *randomness sharing*, legitimate parties probe the reciprocal wireless channel between them. *Information reconciliation* requires the two nodes to communicate with one another to reconcile differences, or non-reciprocities, between their channel measurements. *Privacy amplification* is a process that maps reconciled channel measurements to a key whose maximum size depends on the randomness of the measurements and the amount of information leaked to the eavesdropper. Finally, in *secure communication* the parties transmit messages using the key. This can be done as either a one-time pad or with a symmetric encryption algorithm.

Secure information transmission methods, which also rely on the channel reciprocity between Alice and Bob, make use of the channel state information (CSI) to degrade Eve's channel. Researchers in this field, e.g. [14]–[17], use the CSI between Alice and Bob to encrypt/pre-code the information bits B_i before transmission. When these pre-coded information bits are broadcast by Alice to Bob and Eve, the channel between Alice and Bob acts as a decryptor which (ideally) allows Bob to see the transmitted bits B_i and Eve to obtain $B_i' \neq B_i$.

One secure information transmission solution proposed by Goel and Negi [17] introduces the concept of artificial noise. In this method, the degrees of freedom available in multiple antenna communication systems are utilized to generate artificial noise. The produced artificial noise lies in the null-space of the legitimate user's channel while the information is transmitted in the range space of said channel. Hence, when the channel state information (CSI) is *perfectly* known at both the transmitter and receiver, the legitimate user's channel removes the artificial noise completely. Moreover, for eavesdroppers in different locations who experience their own unique channels, the artificial noise leaks into the eavesdropper's range-space causing a significant toll on the link quality of these users.

In this paper, we propose a secure information transmission system for SS communications that has two parts. First, the reciprocal wireless channel is utilized to derive a pair of spreading gain vectors as keys for the legitimate parties (Alice and Bob). Second, we extend the concept of artificial noise to SS systems. The processing gain of SS systems provides an interesting opportunity to implement a key-based communication system that is *fault-tolerant* - i.e. the communication system allows some tolerance to mismatch in spreading codes used by two legitimate parties.

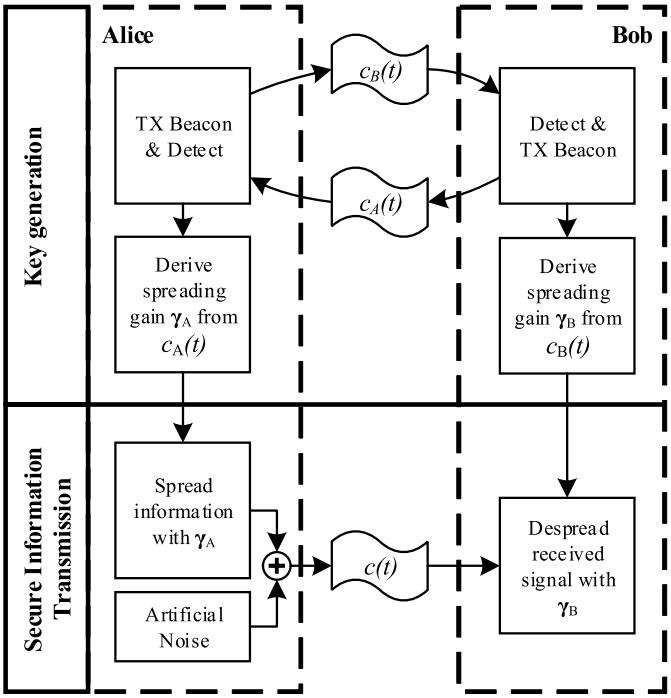

Fig. 1. Block diagram of proposed secure communication system. The paper is organized according to this diagram. Section III details the key generation procedure while Section IV talks about the proposed secure information transmission system.

For secure key generation, we make use of variation in the channel frequency response across the large bandwidth available in SS systems to develop a novel method that leads to generation of similar keys at Alice and Bob's nodes, but a significantly different key at Eve's node. The method is also designed to account for the fact that Alice and Bob's nodes may be time asynchronous with respect to each other. Practicality of the proposed solution is confirmed through a vast set of experimental works.

The second component of the design introduces the concept of artificial noise to SS systems. Discussion of artificial noise in the literature [17]–[19] has largely been in the context of multiple antenna systems. Rather than using multiple antennas to obtain the necessary dimensionality with which to transmit artificial noise, this paper introduces the use of chips in SS for this purpose. The artificial noise is produced in the null-space of the spreading gain vector generated in the secure key generation step.

Fig. 1 shows a block diagram of the proposed secure information transmission system. In the first step, Alice transmits a beacon to Bob who detects it and transmits a beacon back to Alice. Both parties process their received beacons to derive spreading codes from the CSI. In the final step, Alice encodes

confidential information symbols using her spreading code and adds artificial noise before transmission. Bob applies his own spreading code to the received data to remove the artificial noise and subsequently decode the information symbols. Eavesdroppers with significantly different spreading codes fail to recover the information symbols, even if they have a significant SNR advantage, due to the artificial noise. In this paper, we hope to not only present a method to adequately secure SS systems, but also show that SS can be used to provide a robust solution for physical-layer security applications.

This paper is organized as follows. Our adversary model is discussed in Section II. The steps taken to convert the channel measurements to a key are described in Section III. Section IV describes how the keys, along with the added artificial noise, will be utilized for secure information transmission. The security level of the system is studied in Section V. Simulation and experimental results are presented in Section VI and concluding remarks are made in Section VII.

Notations: Our presentation is a mix of continuous-time and discrete-time signals. We use $x(t)$ when reference is made to a continuous time signal, and $x[n]$ when referring to a discrete-time signal. Vectors and matrices are denoted by lowercase and uppercase bold letters. The Hermitian transpose is denoted by $\mathbf{X}^{\mathrm{H}}$ and $||\mathbf{x}||$ is used to denote the Euclidean norm of a vector $\mathbf{x}$.

II. Adversary Model

In our adversary model, we assume Eve is a passive eavesdropper that can estimate the channel between herself and the legitimate parties. Eve knows the key generation algorithm and performs the same steps as Alice and Bob in order to obtain her own key to detect the communicated data transmitted by Alice. Eve can be near the legitimate users, but she cannot be in the exact location of Alice or Bob. For all of our experimental measurements, her antenna is placed 1/3 of a meter away from Bob. Additionally, we assume that Eve cannot jam the communication link between Alice and Bob, nor can she modify messages exchanged by the legitimate parties. Eve cannot cause a man-in-the-middle attack - i.e. our current security solution does not authenticate the nodes. Moreover, it is assumed that the channel is void of interference such that Alice and Bob can obtain reciprocal estimates. It should be noted that while SS systems are typically used because their processing gain allows them to work under harsh channel conditions, we are proposing a technique which uses SS as a means of obtaining extra dimensionality for security purposes.

III. Secure Key Generation

In this section, we discuss how Alice and Bob set up a pair of keys using the reciprocal channel. Key generation is performed by using the measured channel impulse response (CIR). The proposed key generation procedure results in a random vector that will be used as a spreading gain vector in a SS system. The key generation technique emphasizes on the measures that should be taken to assure the dissimilarity of the key generated by Eve with those of Alice and Bob, assuming that Eve is aware of the steps used by Alice and Bob to set their keys.

A. Channel Model

The wireless channel model of interest to us is the commonly used frequency-selective wideband channel model [20]

$$c(t) = \sum_{i \in \mathcal{M}} \alpha_i \, p(t - \tau_i) \tag{1}$$

where $\mathcal{M} = \{0, 1, \ldots, M-1\}$ and M is the number of paths. The parameters α_i and τ_i are the complex gain and delay associated with the i^{th} path and $p(t)$ is the combined responses of the transmit and receive filters. In this paper, we refer to $p(t)$ as the *probing pulse*.

We use (1) to represent the reciprocal channel between Alice and Bob. Eve's channel is represented by

$$c'(t) = \sum_{i \in \mathcal{M}'} \alpha'_i \, p(t - \tau'_i). \tag{2}$$

Considering the *channel independence over space* property, the channel parameters in (1) and (2) are assumed to be independent of each other.

B. Channel Estimation

In this step, Alice and Bob probe and estimate the wireless channel link that connect them together. To avoid interfering with one another, they resort to a time-division duplex (TDD) method in which Alice transmits a beacon packet to Bob who, upon receiving the beacon, immediately transmits the same packet back to Alice.

After the probing stage, channel estimation is carried out using the cyclic channel estimation procedure mentioned in [21]. The chosen transmit beacon is a length N Zadoff-Chu (ZC) sequence [22], [23]. A few periods of the ZC sequence are transmitted, and signal averaging is performed at the receiver for an accurate estimation of the channel. It is worth noting that the ZC sequence has seen widespread use in LTE and UMTS systems [24] due mostly to its special signal processing properties.

The received signal, after demodulation to baseband, is oversampled at a rate which is L times faster than the beacon symbol rate in the ZC sequence. After averaging across multiple periods of the received signal, the L polyphase components of the signal sequence are separated, and the result is passed to the channel estimator. This leads to polyphase components of the channel estimates. These estimates are then interleaved to obtain the samples of the CIR at a sample interval $T_s = T_b/L$, where T_b is the time interval between the beacon symbols in the ZC sequence. This process is performed by Alice, Bob, and Eve, giving each a CIR estimate denoted by $c_{\mathrm{A}}[n]$, $c_{\mathrm{B}}[n]$, $c_{\mathrm{E}}[n]$, respectively. This channel estimation technique is advantageous in that it allows us to obtain the samples of CIR at a high resolution in time with relatively low complexity, [21]. As will be found later, this will become instrumental in the development of an effective key generation algorithm. For a more thorough discussion of the channel estimation step, see [25].

C. Timing and Phase Synchronization

At this point, assuming that the channel is static within the probing interval, Alice and Bob both have their own discrete sample estimates $c_{\mathrm{A}}[n]$ and $c_{\mathrm{B}}[n]$ with three notable differences: 1) Because of the TDD nature of probing, $c_{\mathrm{A}}[n]$ and $c_{\mathrm{B}}[n]$ are subject to a time misalignment; 2) $c_{\mathrm{A}}[n]$ and $c_{\mathrm{B}}[n]$ are affected by different phase errors, arising from the unsynchronized local oscillators (LO) of Alice and Bob, respectively; 3) $c_{\mathrm{A}}[n]$ and $c_{\mathrm{B}}[n]$ are affected differently by the channel noise. We can represent these differences in equation form as

$$c_{\mathrm{A}}[n] = c(nT_s - \mu_{\mathrm{A}})e^{j\theta_{\mathrm{A}}} + \eta_{\mathrm{A}}[n] \tag{3a}$$

$$c_{\mathrm{B}}[n] = c(nT_s - \mu_{\mathrm{B}})e^{j\theta_{\mathrm{B}}} + \eta_{\mathrm{B}}[n] \tag{3b}$$

where μ_{A} and μ_{B} are time delays, θ_{A} and θ_{B} are phase errors, and $\eta_{\mathrm{A}}[n]$ and $\eta_{\mathrm{B}}[n]$ are channel noise terms. The parameters $(\mu_{\mathrm{A}}, \theta_{\mathrm{A}})$ and $(\mu_{\mathrm{B}}, \theta_{\mathrm{B}})$ are, in general, different between Alice and Bob. If these differences are not accounted for, it can lead to a pair of dissimilar keys.

To convert $c_{\mathrm{A}}[n]$ and $c_{\mathrm{B}}[n]$ to a pair of time and phase aligned CIRs, we proceed as follows. For time alignment, the center of the strongest path in both $c_{\mathrm{A}}[n]$ and $c_{\mathrm{B}}[n]$ are identified and shifted to a predefined location. Subsequently, for phase alignment, the elements of both CIRs are normalized with a pair of phase rotations that equalizes the phase of the samples that correspond to the center of the strongest path. This phase alignment procedure returns CIR estimates which have zero phase at the center of their strongest paths.

An early attempt to align $c_{\mathrm{A}}[n]$ and $c_{\mathrm{B}}[n]$ based on the strongest path has been reported in [25]. In this work, the location of the strongest path in $c_{\mathrm{A}}[n]$ and $c_{\mathrm{B}}[n]$ is found independently by both nodes and time aligned to. This procedure may fail in the following scenario. When the CIR of the wireless link between Alice and Bob contains two or more strong paths with similar amplitudes, the presence of the noise terms $\eta_{\mathrm{A}}[n]$ and $\eta_{\mathrm{B}}[n]$ may lead to different locations for the strongest path in $c_{\mathrm{A}}[n]$ and $c_{\mathrm{B}}[n]$. As a result, the generated keys by Alice and Bob may be significantly different. In this paper, we take an approach that allows Bob to time align to Alice's strongest path by using some limited information that he gets (through a public channel) from Alice.

To start, Alice and Bob interpolate their respective CIRs $c_{\mathrm{A}}[n]$ and $c_{\mathrm{B}}[n]$ by a factor of L_2. This further increases the time resolution of the available samples. The remaining steps are performed on these interpolated CIRs which we call $\tilde{c}_{\mathrm{A}}[n]$ and $\tilde{c}_{\mathrm{B}}[n]$ and assume to be good approximations of their respective continuous time function counterparts. In the subsequent discussions, we refer to the length of the interpolated CIRs $\tilde{c}_{\mathrm{A}}[n]$ and $\tilde{c}_{\mathrm{B}}[n]$ as N_c.

After interpolation, both nodes estimate the "path candidates" in their respective CIRs. Path candidates are considered to be a combination of estimated path gains and delays, which are defined for Alice as $\tilde{\alpha}_{i,\mathrm{A}}$ and $\tilde{k}_{i,\mathrm{A}}$, for $i = 0, 1, \cdots, M-1$, and are similarly defined for Bob. These parameters are determined by taking the following steps. Here, we have removed the subscripts A and B for simplicity, but it should be understood that the presented steps are applied to both $\tilde{c}_{\mathrm{A}}[n]$ and $\tilde{c}_{\mathrm{B}}[n]$.

Step 0: Initialize $i = 0$ and $\tilde{c}_i[n] = \tilde{c}[n]$.

Step 1: Let

$$[\tilde{k}_i, \tilde{\alpha}_i] = \arg\min_{\tilde{k}_i, \tilde{\alpha}_i} ||\tilde{c}_i[n] - \tilde{\alpha}_i\, p[n - \tilde{k}_i]||^2. \tag{4}$$

Step 2: Remove path candidate i from the CIR by taking

$$\tilde{c}_{i+1}[n] = \tilde{c}_i[n] - \tilde{\alpha}_i\, p[n - \tilde{k}_i]. \tag{5}$$

Step 3: Increment i by one and repeat **Step 1** and **Step 2** until $i = M$.

Once path candidates $(\tilde{\alpha}_i, \tilde{k}_i)$ are calculated, the interpolated CIRs are time-shifted such that their largest path gain falls to the middle point of respective sequences. Note that this requires adjustment of the delay parameters $\tilde{k}_i$. Subsequently, the mean delay parameter

$$\bar{k} = \left\lfloor \frac{\sum_i \tilde{k}_i |\tilde{\alpha}_i|^2}{\sum_i \tilde{k}_i} \right\rfloor \tag{6}$$

is calculated at both Alice's and Bob's nodes.

Next, Alice calculates the relative time difference between her estimate of the instantaneous mean delay and the location of her strongest path - which had been time aligned to the middle of the CIR. This results in a new delay parameter $k_{\mathrm{D}} = \frac{N_c}{2} - \bar{k}_{\mathrm{A}}$. Alice then transmits k_{D} to Bob. Note that this transmission does not need to be secure as this information has no value to Eve, whose channel has no similarity to Alice's or Bob's channel. Upon receiving k_{D}, Bob calculates the reference delay

$$k_{\mathrm{ref}} = \bar{k}_{\mathrm{B}} + k_{\mathrm{D}}. \tag{7}$$

At this point, k_{ref} should be a time location in Bob's CIR near the strongest path of Alice's CIR. However, non-reciprocities and estimation error in the CIR adds uncertainty to the location of Alice's strongest path relative to Bob's. To handle this issue, we propose that Bob solves the equation

$$[\tilde{k}_{\mathrm{sp,B}}, \tilde{\alpha}_{\mathrm{sp,B}}] = \arg \min_{i \in [0, M-1]} ||p_i[n] - p[n - k_{\mathrm{ref}}]||^2 \tag{8}$$

where $p_i[n] = \tilde{\alpha}_{i,\mathrm{B}}\, p[n - \tilde{k}_{i,\mathrm{B}}]$. Note that (8) searches for the path candidate of Bob's channel which maximally correlates to $p[n - k_{\mathrm{ref}}]$. The corresponding output $\tilde{k}_{i,\mathrm{B}}$ in (8) is then used as Bob's reference point and is thus time aligned to the middle of the respective sequence. This procedure finalizes the time alignment of $\tilde{c}_{\mathrm{A}}[n]$ and $\tilde{c}_{\mathrm{B}}[n]$.

Once $\tilde{c}_{\mathrm{A}}[n]$ and $\tilde{c}_{\mathrm{B}}[n]$ are time aligned, they are circularly shifted so that the center of the strongest path of Alice's CIR and the matching strong path of Bob's CIR will be located at the time index $n = 0$. The results are subsequently decimated L_2-fold to obtain a pair of channel estimates of length NL. Lastly, the channel estimates are phase aligned by introducing a phase shift to the elements of each CIR such that the path located at time index $n = 0$ has phase of zero. We call the final time and phase aligned CIRs $\hat{c}_{\mathrm{A}}[n]$ and $\hat{c}_{\mathrm{B}}[n]$.

D. Strongest Path Cancellation

Now that the timing and phase offsets have been resolved, let us consider a passive adversary, Eve, who follows the exact same synchronization steps as Alice for her own estimated CIR to obtain $\hat{c}_{\mathrm{E}}[n]$. We note that by following Alice's time alignment steps, Eve can better synchronize with the legitimate users than she could by following Bob's alignment procedure. For simplicity, we ignore the channel noise term, and thus the final CIR estimates for Alice and Eve can be expressed as

$$\hat{c}_{\mathrm{A}}[n] = |\tilde{\alpha}_{\mathrm{sp,A}}|\, p[nL_2] + \sum_{i \in \mathcal{M}_{\backslash \mathrm{sp}}} \tilde{\alpha}_{i,\mathrm{A}}\, p[nL_2 - \tilde{k}_{i,\mathrm{A}}] \quad (9)$$

$$\hat{c}_{\mathrm{E}}[n] = |\tilde{\alpha}_{\mathrm{sp,E}}|\, p[nL_2] + \sum_{i \in \mathcal{M}'_{\backslash \mathrm{sp}}} \tilde{\alpha}_{i,\mathrm{E}}\, p[nL_2 - \tilde{k}_{i,\mathrm{E}}] \quad (10)$$

where $\mathcal{M}_{\backslash \mathrm{sp}}$ and $\mathcal{M}'_{\backslash \mathrm{sp}}$ contains the set of all paths excluding the strongest path for Alice and Eve, respectively.

Next, we define the length NL CIR vectors $\hat{\mathbf{c}}_{\mathrm{A}} = \{\hat{c}_{\mathrm{A}}[n]\}$, $\hat{\mathbf{c}}_{\mathrm{B}} = \{\hat{c}_{\mathrm{B}}[n]\}$, and $\hat{\mathbf{c}}_{\mathrm{E}} = \{\hat{c}_{\mathrm{E}}[n]\}$. Also, we let $\mathbf{p} = \{p[n]\}$. Given (9) and (10), the partial correlation between Alice and Eve's CIR estimates can be expressed as

$$\varrho_{\mathrm{AE}} = \frac{\hat{\mathbf{c}}_{\mathrm{A}}^{\mathrm{H}} \hat{\mathbf{c}}_{\mathrm{E}}}{\|\hat{\mathbf{c}}_{\mathrm{A}}\|\, \|\hat{\mathbf{c}}_{\mathrm{E}}\|}. \quad (11)$$

Evaluation of (11) using (9) and (10) gives

$$\varrho_{\mathrm{AE}} = \varrho_{\mathrm{sp,AE}} + \varrho_{\backslash \mathrm{sp,AE}} \quad (12)$$

where

$$\varrho_{\mathrm{sp,AE}} = \frac{|\tilde{\alpha}_{\mathrm{sp,A}}\|\tilde{\alpha}_{\mathrm{sp,E}}|\, \|\, \mathbf{p}^2\|}{\|\hat{\mathbf{c}}_{\mathrm{A}}\|\, \|\hat{\mathbf{c}}_{\mathrm{B}}\|} \quad (13)$$

is a positive and relatively large term arising from the time and phase synchronized strongest paths of Alice and Eve, and $\varrho_{\backslash \mathrm{sp,AE}}$ is the residual partial correlation arising from the remaining paths. Since these remaining paths are not synchronized, their partial correlations are usually a set of zero-mean, low variance random variables that add up to a statistically small value. This observation leads us to the following proposal.

To minimize the similarity of the keys generated by Alice and Bob with the key that Eve generates, Alice and Bob should remove the strongest paths of their respective synchronized CIR estimates and use the residual responses to set the keys. We call this method strongest path cancellation (SPC) and use $\bar{c}_{\mathrm{A}}[n]$, $\bar{c}_{\mathrm{B}}[n]$, and $\bar{c}_{\mathrm{E}}[n]$ to denote the residual CIRs for Alice, Bob, and Eve, respectively. For instance, Alice's CIR after removal of strongest path is obtained as

$$\bar{c}_{\mathrm{A}}[n] = \hat{c}_{\mathrm{A}}[n] - |\tilde{\alpha}_{\mathrm{sp,A}}|\, p[nL_2] \quad (14)$$

and similar equations are used to obtain the residual CIRs of Bob and Eve.

Our assumption here, which has been validated through an extensive set of 32.5 MHz wide indoor wireless channel measurements, has confirmed that the residual CIRs assure highly correlated keys for Alice and Bob, while leading to a dissimilar key for Eve.

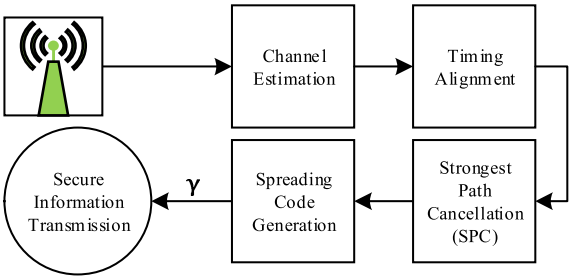

Fig. 2. Block diagram of proposed key generation method in which spreading gains are generated from the channel impulse response.

E. Key Generation

The final step in obtaining a spreading code sequence from the reciprocal wireless channel is outlined here. All parties follow the same procedure as Alice who first takes the DFT of $\bar{c}_{\mathrm{A}}[n]$ and stores it in $\bar{\mathbf{C}}_{\mathrm{A}}$. Next, a key is constructed as

$$\left\{ \gamma_{\mathrm{A}} = \frac{\bar{\mathbf{C}}_{\mathrm{A}}[\mathbf{m}]}{\|\bar{\mathbf{C}}_{\mathrm{A}}[\mathbf{m}]\|} \;\middle|\; \mathbf{m} \in \left[\text{Passband of } \mathbf{C}_{\mathrm{A}}\right] \right\} \quad (15)$$

by Alice. Similarly, Bob and Eve respectively generate γ_{B} and γ_{E}.

At this point, we note that further steps can be taken to build a more secure key. For instance, in [25], the users take the key to be the summation of the phase of the frequency response of the channel with a shuffled version of the same signal. This key has a nice property which further decorrelates Eve's key from the legitimate users' keys. However, after consideration of artificial noise discussed in the following section, we have found more success by simply adopting the passband response of the channel.

The key generation procedure discussed in this section is summarized in Fig. 2. Once obtained, these sequences are used as an integral part of the secure information transmission communication system that is discussed in the following section.

To conclude this section, we would like to point out the following. First, it should be noted that the computational complexity in obtaining the key is relatively low. The main parts of the algorithm are the following operations: match filtering, interpolation, cross-correlation, and the DFT. All of these operations can be solved with a computational cost of $O(N \log N)$, hence, incur a very minimal complexity. Moreover, since the randomness of the key is taken from the channel frequency diversity, the time required to obtain a key remains minimal. For example, in our experiment, it takes approximately 1.1ms for Alice and Bob to exchange their beacons and accordingly set up their keys. Generating multiple keys, uncorrelated to one another, requires a sufficiently dynamic channel and such a condition depends on the coherence time of the channel which is typically on the order of 10 to 100 ms.

IV. Secure Information Transmission

In this section, the proposed secure information transmission system is detailed. First, the mathematical model of

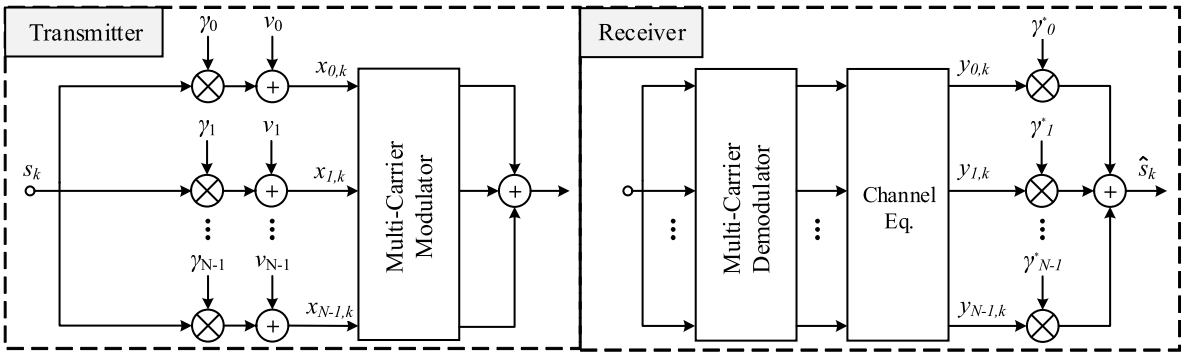

Fig. 3. Block diagram of MC-SS transmitter and receiver with the addition of artificial noise.

the solution is given. Next, we discuss our artificial noise transmit strategy and finally, the security level of the proposed solution is studied. Alice is taken to be the node that wishes to transmit confidential information to Bob, while Eve is a passive eavesdropper listening to Alice's transmit signal. A simplified approach to the physical-layer will be taken so that analysis is straight-forward.

A. MC-SS With Artificial Noise

The secure information transmission system proposed in this section makes use of the chips available to SS systems to produce artificial noise and thus it is easily adoptable to single-antenna systems. This concept differs significantly from those in the literature - e.g. [17]–[19] - that use multiple antennas as means of obtaining the necessary dimensionality with which to produce artificial noise.

To simplify the forthcoming discussion, we will consider MC-SS as the transmit waveform. A block diagram for the proposed MC-SS transmitter with the addition of artificial noise is shown in Fig. 3 along with its corresponding receiver. Note that the receiver does not need additional circuitry to account for the artificial noise since it is removed by the despreader and any residual error due to artificial noise leaking into the information space is taken as additive noise. Additionally, the "Multi-Carrier Modulator" and "Multi-Carrier Demodulator" blocks in Fig. 3 are meant to allow for any MC-SS based waveform design such as OFDM, FB-MC-SS [26], etc. We purposely do not restrict our study to any particular MC-SS based method as the following system model can be easily extended to any MC-SS waveform.

Following the transmitter in Fig. 3, Alice builds a transmit signal using the key from (15) as

$$\mathbf{x}_k = \boldsymbol{\gamma}_{\mathrm{A}} s_k + \mathbf{v}_k \tag{16}$$

where $k = 0, 1, \ldots, K-1$ and $\mathbf{v}_k$ is artificial noise vector, added to increase security in presence of an eavesdropper. The artificial noise $\mathbf{v}_k$ is selected to lie in the null-space of $\boldsymbol{\gamma}_{\mathrm{A}}$, so that $\boldsymbol{\gamma}_{\mathrm{A}}^{\mathrm{H}} \mathbf{v}_k = 0$. More explicitly, $\mathbf{v}_k$ is generated as the residual between an i.i.d circularly symmetric complex Gaussian noise vector $\mathbf{w}_k$ and its projection onto the space of $\boldsymbol{\gamma}_{\mathrm{A}}$ as follows

$$\mathbf{v}_k = \mathbf{w}_k - (\boldsymbol{\gamma}_{\mathrm{A}}^{\mathrm{H}} \mathbf{w}_k) \boldsymbol{\gamma}_{\mathrm{A}}. \tag{17}$$

The total transmit power across the entire occupied bandwidth can be obtained by combining (16) and (17). This gives

$$\begin{aligned} P &= [\mathbf{x}_k^{\mathrm{H}} \mathbf{x}_k] \\ &= \sigma_s^2 + \frac{N-1}{N} \sigma_w^2 \end{aligned} \tag{18}$$

where

$$\sigma_w^2 = [\mathbf{w}_k^{\mathrm{H}} \mathbf{w}_k] \tag{19}$$

and the factor $\frac{N-1}{N}$ arises from the fact that the artificial noise is generated from a complete N-dimensional vector space with one of its dimensions removed. We denote the fraction of power allocated to the information signal as ϕ. This implies that

$$\sigma_s^2 = \phi P \tag{20}$$

$$\sigma_w^2 = \frac{(1-\phi) N P}{N-1}. \tag{21}$$

Following (16), the signal received by Bob and Eve *after* multi-carrier demodulation and application of a zero-forcing channel equalizer are respectively given by

$$\mathbf{y}_k = \mathbf{x}_k + \boldsymbol{\eta}_k \tag{22}$$

$$\mathbf{z}_k = \mathbf{x}_k + \boldsymbol{\epsilon}_k \tag{23}$$

where the components of $\boldsymbol{\eta}_k$ and $\boldsymbol{\epsilon}_k$ arise from channel noise. Note that the elements of $\boldsymbol{\eta}_k$ and $\boldsymbol{\epsilon}_k$ may not be i.i.d due to frequency selectivity of the channel. The SNR at the Alice-Bob link and Alice-Eve link, thus, can be expressed as

$$\mathrm{SNR}_{\mathrm{B}}^{\mathrm{i}} = \frac{P}{\sigma_\eta^2} \tag{24}$$

$$\mathrm{SNR}_{\mathrm{E}}^{\mathrm{i}} = \frac{P}{\sigma_\epsilon^2} \tag{25}$$

where $\sigma_\eta^2 = [\boldsymbol{\eta}_k^{\mathrm{H}} \boldsymbol{\eta}_k]$ and $\sigma_\epsilon^2 = [\boldsymbol{\epsilon}_k^{\mathrm{H}} \boldsymbol{\epsilon}_k]$. Note that the superscript 'i' is added to the SNR terms to emphasize that these are at the receiver input. Next, Bob and Eve despread their received signals from (22) and (23) with their own spreading gains to get

$$\boldsymbol{\gamma}_{\mathrm{B}}^{\mathrm{H}} \mathbf{y}_k = \boldsymbol{\gamma}_{\mathrm{B}}^{\mathrm{H}} \boldsymbol{\gamma}_{\mathrm{A}} s_k + \boldsymbol{\gamma}_{\mathrm{B}}^{\mathrm{H}} \mathbf{v}_k + \boldsymbol{\gamma}_{\mathrm{B}}^{\mathrm{H}} \boldsymbol{\eta}_k \tag{26}$$

$$\boldsymbol{\gamma}_{\mathrm{E}}^{\mathrm{H}} \mathbf{z}_k = \boldsymbol{\gamma}_{\mathrm{E}}^{\mathrm{H}} \boldsymbol{\gamma}_{\mathrm{A}} s_k + \boldsymbol{\gamma}_{\mathrm{E}}^{\mathrm{H}} \mathbf{v}_k + \boldsymbol{\gamma}_{\mathrm{E}}^{\mathrm{H}} \boldsymbol{\epsilon}_k. \tag{27}$$

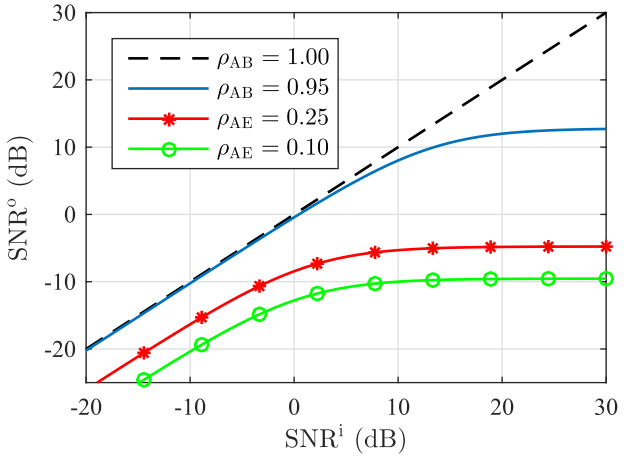

Fig. 4. Plot of the SNR after despreading versus receiver SNR for $\phi = 1/N$ and selected values of ρ_{AB} and ρ_{AE}.

The SNR at Bob's node after the despreader is derived in an appendix at the end of this paper and is found to be

$$\mathrm{SNR}_B^o = \frac{N\phi\rho_{AB}\mathrm{SNR}_B^i}{\frac{N}{N-1}(1-\phi)(1-\rho_{AB})\mathrm{SNR}_B^i + 1} + 1. \tag{28}$$

where

$$\rho_{AB} = |\boldsymbol{\gamma}_B^H \boldsymbol{\gamma}_A|^2 \tag{29}$$

and the superscript 'o' is added to the SNR terms to emphasize that it is at the output, i.e., after the despreader. Equations (28) and (29) are defined similarly for the Alice-Eve link with the appropriate substitutions.

When there is no artificial noise, i.e. $\phi = 1$, (28) reduces to $\mathrm{SNR}_B^o = N\rho_{AB}\mathrm{SNR}_B^i$. This shows that the despreading procedure, through coherent linear combination of the received signal vector, allows Bob to achieve an SNR up to N times the link SNR in (24). On the other hand, if Eve can gain access to the spreading code $\boldsymbol{\gamma}_A$, she can decode the information symbols sent by Alice. This highlights the necessity of the algorithm discussed in Section III where Alice and Bob make use of the reciprocal wireless channel to generate a pair of similar keys while Eve, despite following the same steps as the legitimate nodes, generates a significantly different key.

To enlighten the reader on how artificial noise can be used to boost security, we plot SNR_B^o and SNR_E^o as a function of the received signal SNR at $\phi = 1/N$ in Fig. 4. We use the terms SNR^i and SNR^o to respectively describe the SNR before and after despreading at either Bob or Eve's node, depending on the context. The values of ρ_{AB} and ρ_{AE} were chosen arbitrarily to show that when Alice and Bob share nearly identical keys, they have a significant SNR advantage compared to the adversary who generates a different key.

B. Artificial Noise Transmit Strategy

An important parameter for artificial noise transmission systems is the signal-to-artificial noise ratio ϕ. In [17], this parameter is found through maximization of the secrecy capacity - defined as the maximum rate at which Alice-Bob can communicate a message without an eavesdropper being able to decode it. This power allocation strategy is applicable only when Alice has perfect knowledge of the full CSI - e.g. the CSI between herself and Bob and herself and Eve. Since the knowledge of perfect CSI between Bob and Eve is not possible in practice, this method of selection of the artificial noise power may be only of interest from a theoretical point of view.

Here, we are interested in practical scenarios where Eve's CSI is not known to Alice. In this case, secrecy cannot be guaranteed as Alice does not know how much artificial noise to inject to Eve's channel. With the assumption of Eve's CSI remaining unkown, an approach taken in [18] selects ϕ to meet a target SNR at Bob's node, assuming that the Alice-Bob CSI is perfectly known. The rest of the available transmit power is devoted to artificial noise, hoping this will sufficiently deteriorate Eve's channel such that she will not be able to decode the transmit message

Our power allocation strategy follows the same idea of dedicating enough power to the information subspace to ensure a certain link quality between Alice and Bob. However, we do not make the assumption that perfect knowledge of Alice-Bob CSI is available. Instead, we propose an artificial noise power allocation strategy in which Alice dedicates enough power to the information to ensure a target SNR is met for Bob so long as the similarity of their keys - quantified by ρ_{AB} - is larger than a threshold $\rho_{\min}$.

The parameter ϕ for our signal-to-artificial noise power allocation strategy can be determined by replacing SNR_B^o in (28) with a target SNR - SNR_T^o - and ρ_{AB} with threshold $\rho_{\min}$. Solving for ϕ with these substitutions in place gives

$$\phi = \frac{\frac{N}{N-1}(1-\rho_{\min})\mathrm{SNR}_B^i + 1}{\frac{N}{N-1}(1-\rho_{\min})\mathrm{SNR}_B^i + N\rho_{\min}\frac{\mathrm{SNR}_B^i}{\mathrm{SNR}_T^o}}. \tag{30}$$

As a check, note that if the spreading codes are assumed perfectly known by Alice and Bob, hence, $\rho_{\min} = 1$, the above reduces to the same result reported in [18].

One point to note here is that there is a limit to how low $\rho_{\min}$ can be set for a given SNR_T^o and $\phi_{\min}$ - defined as the smallest signal-to-artificial noise ratio that a designer would consider. To determine this limit, we set $\phi = \phi_{\min}$ in (30) and solve for $\rho_{\min}$ to get

$$\lim_{\mathrm{SNR}_B^i \to \infty} \rho_{\min} = \frac{\mathrm{SNR}_T^o(1-\phi_{\min})}{\mathrm{SNR}_T^o(1-\phi_{\min}) + (N-1)\phi_{\min}}. \tag{31}$$

V. Security Level of Proposed Solution

This section evaluates the security level of our solution. Three different attack scenarios are discussed in this section. The first two of these attacks are studied thoroughly, while the third one is mentioned as a subject for future study.

A. Scenario 1: The Passive Eavesdropper

For the first attack scenario, Eve is a passive eavesdropper who tries to decode Alice's transmitted information symbols using the key generated by herself. Eve is equipped with the same receiver as Bob and the only difference between them is in their spreading codes.

To evaluate the security level of this attack, we first consider the use of the popular secrecy characterization from [27], where the notion of secrecy outage probability is expressed as

$$\mathcal{P}_{\text{out}}(R_s) = \mathcal{P}\left(C_{\text{B}} - C_{\text{E}} < R_s\right) \tag{32}$$

where $C_{\text{B}} = \log_2(1 + \text{SNR}_{\text{B}}^{\text{o}})$, $C_{\text{E}} = \log_2(1 + \text{SNR}_{\text{E}}^{\text{o}})$.

The definition in (32) makes an assumption that the transmitter chooses a strategy that leads to the main-link communicating near capacity of the channel. In this way, while $\text{SNR}_{\text{B}}^{\text{o}}$ will allow for sufficient information recovery at Bob's node, $\text{SNR}_{\text{E}}^{\text{o}}$ will be inadequate in decoding information at Eve's node. The parameter R_s is effectively a margin that when chosen larger, increases the secrecy outage probability. An outage occurs when a message is either unreliable for Bob to decode or insecure - i.e. there is a possibility that Eve decodes the message.

A known weakness of the secrecy characterization by (32) was discussed in [28]. It was noted that (32) does not distinguish between reliability and security. The secrecy outage probability may be minimized for a given set of design parameters, but it is not obvious from (32) whether this is due to an information leak or a reliability issue.

Accordingly, the following alternative definition of secrecy outage probability was proposed. The outage was defined for when the difference between the target capacity and Eve's capacity is lower than R_s, conditioned on the event that a message was transmitted. In our model, we assume that message transmission always occurs since Alice and Bob are operating independent of one another. The secrecy outage probability definition from [28] is thus modified as

$$\mathcal{P}_{\text{out}}(R_s) = \mathcal{P}\left(R_{\text{T}} - C_{\text{E}} < R_s\right) \tag{33}$$

where $R_{\text{T}} = \log_2(1 + \text{SNR}_{\text{T}}^{\text{o}})$.

The definition of (33) states that an outage occurs when Eve's SNR after despreading is within the margin of R_s from the target rate R_{T}. The characterization in (33) is useful from a practical standpoint in which Alice and Bob are operating independent of one another. In such a case, Alice chooses a code that optimally works (i.e. error-free) for target rate R_{T}. This is different from the characterization in (32) where it is implied that if $\text{SNR}_{\text{B}}^{\text{o}} > \text{SNR}_{\text{T}}^{\text{o}}$, Alice chooses a different code to work at rate C_{B} rather than the target rate R_{T}. It also follows that if Alice and Bob are communicating near target rate R_{T}, an appropriate definition for an information leak is the scenario in which C_{E} is near R_{T} rather than the case where C_{E} is close to C_{B}.

With regards to the reliability of the main-link, a nice feature of our artificial noise power allocation strategy is that it assures a target SNR is met so long as the similarity between the keys generated by Alice and Bob is above a threshold. In other words, it can be easily verified that if ϕ is obtained from (30), then $\mathcal{P}(\text{SNR}_{\text{B}}^{\text{o}} < \text{SNR}_{\text{T}}^{\text{o}})$ is equal to $\mathcal{P}(\rho_{\text{AB}} < \rho_{\min})$.

B. Scenario 2: The Sophisticated Eavesdropper

In this attack scenario, Eve is given a significant advantage in decoding the transmitted data. In traditional artificial noise systems, e.g. [17]–[19], the assumption of a block-fading channel model limits the number of symbols that can be transmitted confidentially. In our system, we can transmit as many symbols as needed with a given spreading code since the channel does not directly decrypt the information. The consequence of encoding many symbols with the same key is that a sophisticated adversary may use a *blind method* to identify the information signal subspace and subsequently use that knowledge to decode the communicated data.

Without artificial noise (i.e. $\phi = 1$), secrecy against knowledgeable adversaries could *only* exist for our system model if 1) Eve is at an SNR disadvantage compared to the main-link or 2) Alice only transmits one symbol per key, effectively applying a one-time pad to the solution, provided that the key is generated at channel coherence time intervals. Both of these assumptions are considerably strong to impose on the security of a wireless communication network. Here, we study the use of artificial noise as a way to increase throughput of the secure communication system without assuming Eve to be at a disadvantage.

This attack scenario considers the situation where Alice transmits K symbols with the same spreading code and Eve seeks to estimate $\boldsymbol{\gamma}_{\text{A}}$ from her received signal. To facilitate this study, we redefine (23) as a matrix of concatenated received signal vectors spread with the same key

$$\begin{aligned}\mathbf{Z} &= \left[\mathbf{z}_0\ \mathbf{z}_1\ \ldots\ \mathbf{z}_{K-1}\right] \\ &= \left[\mathbf{x}_0 + \boldsymbol{\epsilon}_0\ \mathbf{x}_1 + \boldsymbol{\epsilon}_1\ \ldots\ \mathbf{x}_{K-1} + \boldsymbol{\epsilon}_{K-1}.\right]\end{aligned} \tag{34}$$

The columns of $\mathbf{Z}$ are a set of random vectors. Each of these vectors have the average energy/power of P and the form of (23). There is a fixed direction $\boldsymbol{\gamma}_{\text{A}}$ that carries data symbols with the power ϕP. The rest of the power is in a random direction perpendicular to $\boldsymbol{\gamma}_{\text{A}}$. When $\phi = 1/N$, the signal power in equally distributed in all directions, including the direction $\boldsymbol{\gamma}_{\text{A}}$. In this scenario, the signal space will appear to be white with respect to all directions, including the data direction, making it hard for an observer that wishes to find $\boldsymbol{\gamma}_{\text{A}}$. The situation will be different when $\phi \neq 1/N$. In such cases, the intruder can search for the direction that carries a different power than the remaining directions.

The standard solution to find the signal direction, i.e., the spreading gain vector $\boldsymbol{\gamma}_{\text{A}}$, when $\phi > 1/N$, is the following.

1) Construct the $N \times N$ matrix

$$\mathbf{R}_{\mathbf{ZZ}} = \frac{\mathbf{1}}{\mathbf{K}}\mathbf{Z}\mathbf{Z}^{\text{H}} \tag{35}$$

2) Invoking the Rayleigh-Ritz Theorem [29] an estimate of $\boldsymbol{\gamma}_{\text{A}}$ is obtained by solving the following maximization problem

$$\hat{\boldsymbol{\gamma}}_A = \arg \max_{||\boldsymbol{\gamma}||=1} \boldsymbol{\gamma}^{\text{H}}\mathbf{R}_{\mathbf{ZZ}}\boldsymbol{\gamma} \tag{36}$$

For this procedure to give an accurate estimate, the number of signal samples (i.e., the parameter K) should be sufficiently large. To give an idea of how how large K should be to obtain a reasonable estimate of $\boldsymbol{\gamma}_{\text{A}}$, we resort to some numerical results which are presented in the next section.

C. Scenario 3: The Brute-Force Attack Eavesdropper

The two passive eavesdropper attacks discussed so far may not necessarily encompass all possible attacks on the proposed

system. Another feasible attack that a passive Eve may use is a brute-force attack. In this attack, Eve takes her received signal vector and guesses multiple different CIRs in an attempt to find one that aligns closest to the information-bearing signal space.

The current key generation technique generates a key of length N using the frequency response of a CIR measurement. If the key generated by Alice and Bob has N' mutual information bits, then Eve - using a brute-force attack - needs to try *up to* $2^{N'}$ CIRs to obtain a sufficient estimate for the key that will remove the artificial noise. Note that the amount of CIRs Eve would need to try depends on many things including the SNR between the main-link, the level of fault-tolerance Alice builds in her transmit signal, the amount of randomness in the key Alice and Bob generate, etc. Additionally, the key discussed in our paper is a very simple one that is sufficient for our study. Another option for generating the key would be to take an approach where Alice and Bob use multiple CIRs - sampled at coherence time intervals - to generate a key that is more random than the one discussed in this report. With such a key, the computational complexity of a brute-force attack can be significantly increased, making the task of a brute force attack very demanding. In light of the intricacies associated with this attack, its detailed study is beyond the scope of this paper and remains a problem for future research.

VI. Results

The proposed key generation and secure information transmission system are tested in this section. Simulation results are presented so that results can be repeated, confirmed, and numerically evaluated. Additionally, experimentation results are provided to validate the performance of the proposed system in real-world environments.

A. Key Generation

1) Simulation Results: To show how well the proposed key generation algorithm uses both time and amplitude to its advantage, we run a simulation. The parameters chosen for the simulation match the experiment. For the simulation, we assume a block fading channel model and no fractional timing offset for all three parties. Given this setup, Monte Carlo simulations were processed according to the following procedure.

1) Alice and Bob generate a probing beacon consisting of 25 periods of a length $N = 64$ ZC sequence. This is interpolated by a factor of $L = 4$ using a square-root raised-cosine filter with a roll-off factor of 1/2 and transmitted at a sampling rate of $\frac{1}{T_s} = 130$MHz.
2) The beacon is transmitted across a simulated wireless channel. The channel follows an exponential power delay profile [20] with delay spread of 50 ns, sampled at uniform intervals of LT_s. The complex gain of each multipath component is Rayleigh faded and the total number of effective multipaths is set to $M = \lfloor 10 \times \frac{50 \text{ ns}}{LT_s} \rceil = 16$. Alice and Bob share the same channel and the only difference between the Alice-Bob and Alice-Eve's channels are the M complex-valued gains.

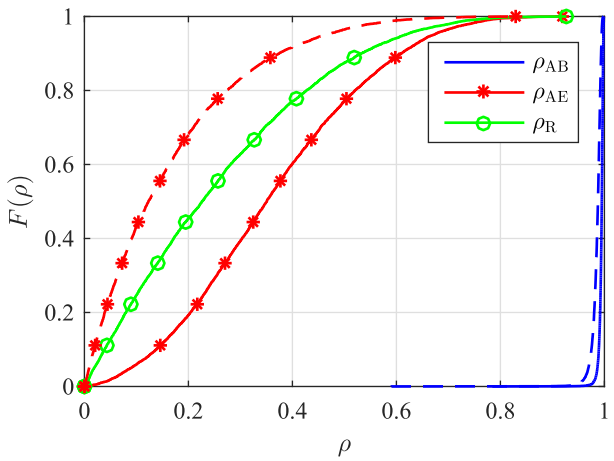

Fig. 5. CDF of partial correlation between Alice and Bob's keys ρ_{AB} and Alice and Eve's keys ρ_{AE} from simulation results using a channel model in which path gains are derived from an exponential power delay profile with RMS delay spread of 50ns. Dashed lines show results after SPC is applied. Additionally, ρ_R shows the partial correlation between the M complex-valued gains of Alice-Bob and Alice-Eve channels.

3) Noise is independently added to the signal received by Alice, Bob, and Eve.
4) Channel estimation, time alignment, and key generation are processed according to the procedure described in Section III. Note that for time alignment, Eve time aligns according to her own strongest path as she has more similarity to the Alice-Bob channel with this approach.

Fig. 5 shows the cumulative distribution function (CDF) of ρ_{AB} and ρ_{AE} before and after SPC from 10,000 runs of the described simulation. Alice and Bob have an SNR of 10 dB, while Eve has zero additive noise in her received signal. In addition to these curves, the partial correlation between the M complex gains of the Alice-Bob and Alice-Eve's channels are also plotted and is denoted by ρ_R.

A few interesting aspects of the proposed key generation algorithm can be found in Fig. 5. First, as expected, a slight decorrelation occurs between Alice and Bob's keys after SPC due to removal of the strongest path. However, this decorrelation is small. In fact, the average value of ρ_{AB} before and after SPC at the present SNR of 10 dB is 0.994 and 0.985, respectively.

Next, consider the curves depicted in Fig. 5 which show the partial correlation between Alice and Eve's keys before and after SPC, as well as the parameter ρ_R. First, it can be seen that before SPC, timing and phase recovery causes Alice and Eve's keys to be relatively strongly correlated. However, after SPC, the partial correlation bias due to time and phase synchronization in (13) is removed and thus the similarity between the keys is significantly less.

Perhaps the most interesting aspect here is that after SPC, ρ_{AE} is statistically much smaller than ρ_R despite the fact that 1) the time-delays of each multipath component are the same for all channels and 2) there is one less source of randomness due to removal of the strongest path. The reason for this is because after time alignment according to the strongest path, the time delays relative to the strongest path

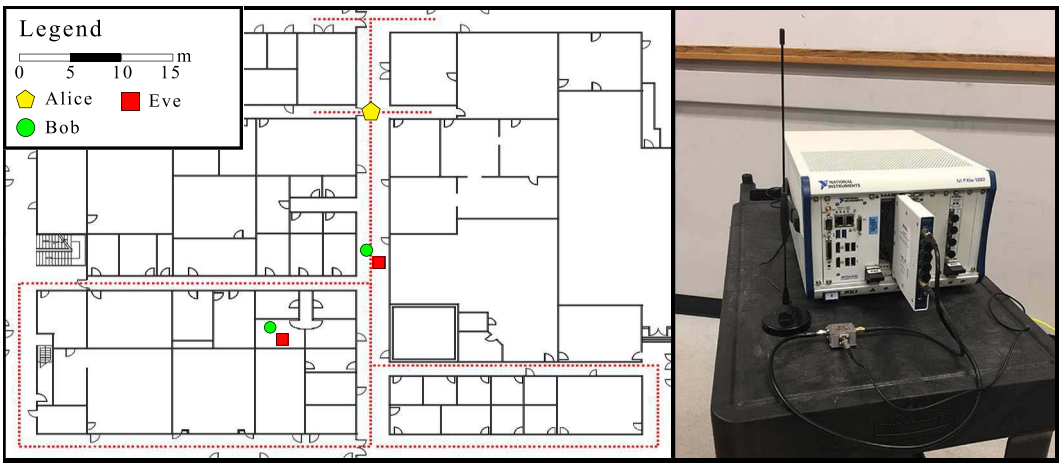

Fig. 6. The picture on the left shows a map of the third floor of Merrill Engineering Building at the University of Utah where the experiment was conducted. The position of Alice was varied across the dotted lines while Bob and Eve remained stationary in one of the two displayed locations. Eve was synchronized to Bob's clock, while Alice and Bob operated on asynchronous clocks. The antenna of Bob and Eve were placed approximately 1/3 meter apart. The right side picture shows one of the three nodes used in our experiment.

are different between the Alice-Bob and Alice-Eve channels. After removing the strongest path, the remaining multipaths add an additional secret - the time delays of the residuals paths relative to the strongest.

Ultimately, Fig. 5 shows that the time delays, in combination with the complex-valued gains of the channel, allow Alice and Bob to share a stronger secret than they would if *only* the complex gains of the channel were used for key generation.

2) Experimental Results: The experiment is run on a transceiver based on the National Instruments (NI) platform. The transceiver consists of an NI FlexRIO FPGA Module (NI PXIe-7975R). This module is connected to an NI FlexRIO RF Transeiver (NI 5791R), which has a sampling rate of 130 MHz. The FPGA and Transceiver module are both connected to an NI real-time controller (NI PXIe-1082), which is used as a host PC and is programmed using NI LabVIEW Real-Time. The FlexRIO RF Transceiver is connected to a circulator (Model No. CS-0.900) that is fed to an RF amplifier (NI PXI-5691) and then to a single antenna. All three parties in our experiment (Alice, Bob, and Eve) use identical transceiver setups and Eve's transmitter is turned off. Experiments are run at a carrier frequency of 900 MHz.

Time-division duplexing is used for channel probing. The duration of each transmitted packet, consisting of multiple repetitions of the ZC sequence is 118μs. A few extra ZC sequences are prepended to the packet for packet detection purposes. The time duration between the time it takes for Alice to measure Bob's channel and vice versa is $\sim$ 1 ms.

Details of the experimental setup are explained in Fig. 6. In total, 6500 channel measurements are captured. Prior to obtaining each measurement, the environment around Alice is varied, either by moving Alice or having an experimenter move around the node to ensure variation between measurements. Data is collected from over-the-air measurements and subsequently used to generate keys offline.

Fig. 7 shows the CDF of ρ_{AB} and ρ_{AE} before and after SPC from the experimental data. Similar to Fig. 5, we see a slight decorrelation between Alice and Bob's keys after

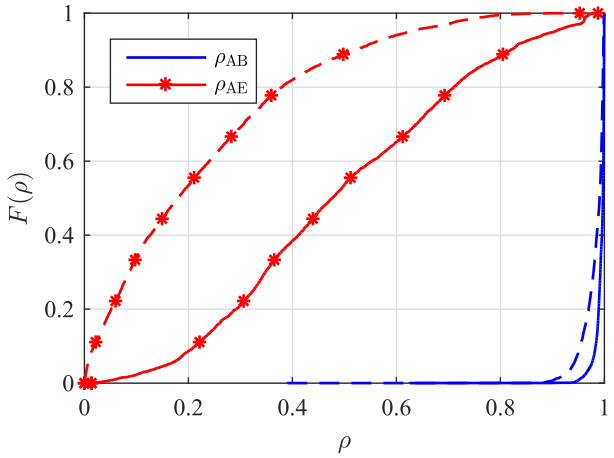

Fig. 7. CDF of partial correlation between Alice and Bob's keys ρ_{AB} and Alice and Eve's keys ρ_{AE} from over-the-air data obtained from the experiment whose setup is shown in Fig. 6. Dashed lines show results after SPC is applied.

SPC as well as a significant increase of dissimilarity between Alice and Eve's keys. Results shown in Fig. 5 and Fig. 7 are fairly similar, though over-the air measurements show Alice and Eve's keys to be slightly more correlated in the experiment than in the simulation. A possible cause for this is that the channel model used in our simulation contains more randomness and/or paths than observed in the measurements. Fig. 5 and Fig. 7 indicate that Eve's key has been decorrelated through SPC. However, the question looming at this point is whether this is worth the reduction in similarity between Alice and Bob's keys. In the following section, we examine this very point. In addition, we recognize that the correlation between the elements within N-length key is high. We find, remarkably, that this matters less when a large amount of artificial noise is used.

B. Secure Information Transmission

The secure information transmission system that we propose adds artificial noise to the traditional MC-SS as a means of

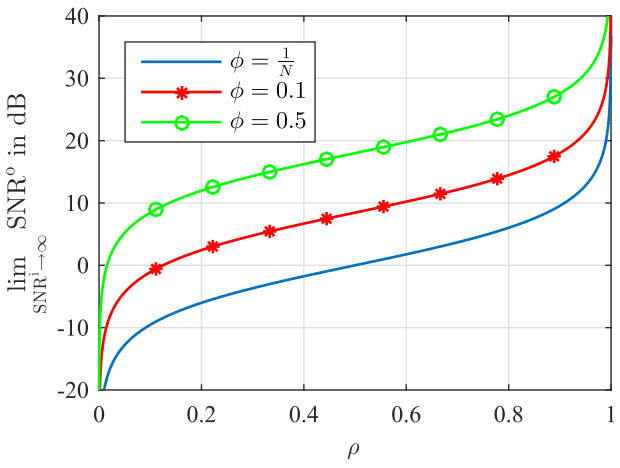

Fig. 8. Plot of the SNR after despreading - $\mathrm{SNR}^{\mathrm{o}}$ - as link SNR approaches infinity as a function of ρ - a measure of similarity between Alice and Bob's keys - for selected values of ϕ.

enhancing physical layer security. At this point, we turn our attention to validating the security of the proposed system and its expected performance for the legitimate parties. We take $N = 64$ since it is the value of N that was used in our key generation experiments as well as in our current implementation of the FB-MC-SS system in [30].

We consider the limit of (28) as the SNR approaches infinity. To simplify the discussion here, we define $\mathrm{SNR}^{\mathrm{o}}$ in (28) as the despreaded signal SNR at Bob or Eve's link. Similarly, $\mathrm{SNR}^{\mathrm{i}}$ and ρ respectively from (24) and (29) are defined in this way. Using L'Hospital's Rule,

$$\lim_{\mathrm{SNR}^{\mathrm{i}}\to\infty} \mathrm{SNR}^{\mathrm{o}} = \frac{(N-1)\phi\rho}{(1-\phi)(1-\rho)}. \tag{37}$$

It is trivial to see from (37) that if no artificial noise is used (i.e. $\phi = 1$) and as $\mathrm{SNR}^{\mathrm{i}}_{\mathrm{E}} \to \infty$, $\mathrm{SNR}^{\mathrm{o}}_{\mathrm{E}}$ will also increase to infinity, hence, no secrecy can be guaranteed regardless of how dissimilar Alice and Eve's keys are. However, the addition of artificial noise (i.e. when ϕ drops below one) provides an intriguing opportunity to securely transmit confidential information despite Eve having a significant SNR advantage. Fig. 8 plots (37) as a function of ρ for different values of ϕ.

In previous literature of artificial noise, where perfect CSI knowledge is assumed (i.e. $\rho_{\mathrm{AB}} = 1$), high values of secrecy data rates can be achieved. However, as it can be seen in Fig. 8, if $\rho_{\mathrm{AB}} < 1$, there is an exponential drop in $\mathrm{SNR}^{\mathrm{o}}_{\mathrm{B}}$ which can lead to a significant data reliability issue that get exacerbated as artificial noise power is increased. This highlights the main advantage of our artificial noise power allocation strategy in (30) because it compensates for dissimilarity between Alice and Bob's keys by strategically introducing enough artificial noise such that a target rate is hit for a given $\rho_{\min}$ that fits the criteria of (31).

In Fig. 8, it can also be seen that the limit of the despreaded signal's SNR linearly increases for $\{\rho \mid 0.2 < \rho < 0.8\}$. Moreover, (37) asymptotically approaches infinity as $\rho \to 1$ and approaches zero as $\rho \to 0$. In short, this trend is encouraging as it shows that the introduction of artificial noise allows for nodes with the "right" key to reliably decode the confidential information while it hampers the decoding ability of users with different keys, even when they have a considerable SNR advantage.

Next, we discuss the two scenarios discussed in Section V.

1) Scenario 1: The Passive Eavesdropper: Results from the simulations and experiments in Section VI-A are used to evaluate the key generation procedure in the context of the proposed secure information transmission system. Two sets of keys will be compared: the key generated before SPC and the key after applying SPC.

As discussed before, Eve follows the same steps as the main-link in retrieving Alice's transmitted data. The effectiveness of this attack is evaluated using the secrecy outage probability in (33). To ensure fair comparison between the two sets of keys, $\rho_{\min}$ is set so that 95% of the keys used will meet the target SNR after despreading, i.e., $\mathcal{P}(\mathrm{SNR}^{\mathrm{o}}_{\mathrm{B}} < \mathrm{SNR}^{\mathrm{o}}_{\mathrm{T}}) = \mathcal{P}(\rho_{\mathrm{AB}} < \rho_{\min}) = 5\%$.

In this way, $\rho_{\min}$ will be smaller for the keys that use SPC due to the slight decorrelation effect that SPC has on the keys. In turn, this means less artificial noise can be added for the keys obtained using SPC. Note that this formulation uses *a-priori* knowledge of ρ_{AB} to determine $\rho_{\min}$, but this is only used to ensure a fair comparison between the two sets of keys. In practice, when *a-priori* knowledge is not available, $\rho_{\min}$ should be set differently. A method that we propose for this practical scenario is detailed in [31].

The secure information transmission strategy we propose is one in which the target rate is adapted according to $\mathrm{SNR}^{\mathrm{i}}_{\mathrm{B}}$. For the adaptive target rate strategy, when $\mathrm{SNR}^{\mathrm{i}}_{\mathrm{B}}$ is too low to meet a minimum target rate $R_{\mathrm{T}\min}$ at $\phi = 1/N$, the signal to artificial noise ratio is calculated using (30). When the SNR at Bob's receiver is high enough and thus a large amount of artificial noise power can be added (i.e. $\phi = \phi_{\min} = 1/N$), then the target rate is increased. To find the target rate in this scenario, we first solve for $\mathrm{SNR}^{\mathrm{o}}_{\mathrm{T}}$ in (30) at $\phi = 1/N$ to obtain

$$\mathrm{SNR}^{\mathrm{o}}_{\mathrm{T}} = \frac{\mathrm{SNR}^{\mathrm{i}}_{\mathrm{B}}\rho_{\min}}{1 + \mathrm{SNR}^{\mathrm{i}}_{\mathrm{B}}(1-\rho_{\min})} \tag{38}$$

and use this to calculate R_{T}.

Fig. 9 shows evaluation of (33) at $R_s = 1$ for the passive eavesdropper attack for simulation and experimental results when using the adaptive target rate strategy. The solid lines correspond to before SPC and the dashed lines correspond to after SPC. To generate this figure, we assume a worst-case scenario where Eve has *zero additive noise* at the receiver. The minimum target rate $R_{\mathrm{T}\min}$ is set to 2 bits and is incremented according to $\mathrm{SNR}^{\mathrm{i}}_{\mathrm{B}}$. Additionally, a reliability of 95% at the main-link is met for all SNR values in Fig. 9. Note that to guarantee this reliability, the smallest value for $\mathrm{SNR}^{\mathrm{i}}_{\mathrm{B}}$ corresponds to $\phi = 1$ for the keys applied with SPC. Below the minimum value of $\mathrm{SNR}^{\mathrm{i}}_{\mathrm{B}}$, there is not enough transmit power at Alice's node to allow for the minimum target rate of 2 bits.

Results from Fig. 9 indicate that the keys derived using SPC provide a significant boost to the security of the system. This is despite the fact that less artificial noise is being broadcast at lower SNR values (i.e. the $\mathrm{SNR}^{\mathrm{i}}_{\mathrm{B}}$ values to the left of the black circles) as a result of the way $\rho_{\min}$ was obtained. It can

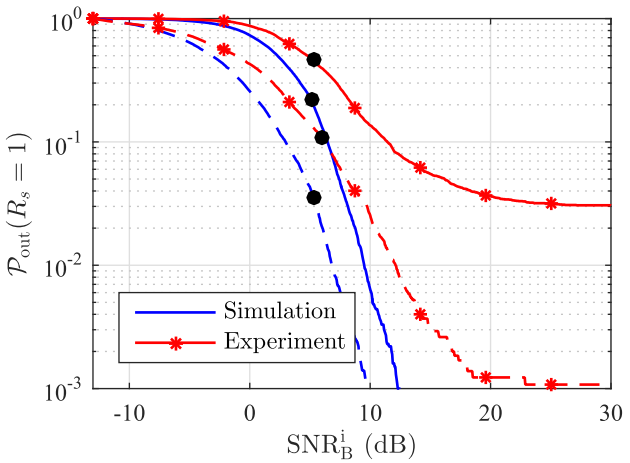

Fig. 9. Plot of the outage probability of secrecy evaluated at $R_s = 1$ as a function of receiver SNR for the adaptive target rate strategy. The plot was obtained using the ρ_{AB} and ρ_{AE} values from keys obtained through simulation and experiment. Dashed lines show keys after SPC is applied. Black circles indicate the transition point at which the target rate R_{T} starts increasing and $\phi = 1/N$.

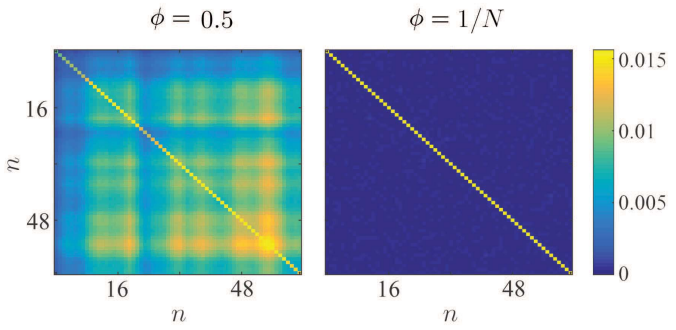

Fig. 10. Plot of the magnitude of covariance matrix of $\mathbf{x}_k$ for one $\boldsymbol{\gamma}_{\text{A}}$ from the experiment data set for $\phi = 0.5$ and $\phi = 1/N$.

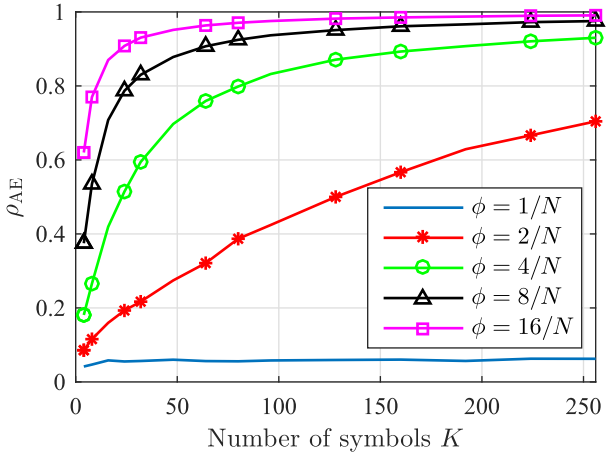

Fig. 11. Plot of the 99th percentile of ρ_{AE} as a function of K. Note that the 99th percentile indicates that 99% of the time, ρ_{AE} is below the lines indicated in the graph

also be seen that when $\text{SNR}_{\text{B}}^{\text{i}}$ is high and $\phi = 1/N$, the probability of secrecy outage approaches a steady state. For the experiment data set, the steady state value for the secrecy outage probability is $\approx 3\%$ for keys that do not use SPC, while keys applied with SPC are $\approx 0.1\%$. Therefore, the minimum amount of security is better with SPC than without. Finally, we note that this transmit strategy allows us to use high levels of artificial noise power ($\phi = 1/N$), which is not only good for securing communications from a secrecy outage standpoint but also beneficial in thwarting the efforts of a more sophisticated adversary that we discuss next.

2) Scenario 2: The Sophisticated Eavesdropper: In this section, we show two different sets of results pertaining to the case wherein multiple symbols are transmitted with the same spreading code sequence. First, we examine the transmitted sequence correlation matrix and show that although there is correlation between elements in the key, it matters less as artificial noise power is increased. Next, we examine the number of symbols that can be transmitted with one key as artificial noise power is varied.

First, consider the transmitted data vector $\mathbf{x}_k$ from (16). It is trivial to show that the covariance matrix of this signal, for a given $\boldsymbol{\gamma}_{\text{A}}$, can be represented as

$$[\mathbf{x}_k \mathbf{x}_k^{\text{H}}] = \frac{1}{N}\sigma_w^2 \mathbf{I}_{\text{N}} + \left(\sigma_s^2 - \frac{1}{N}\sigma_w^2\right)\boldsymbol{\gamma}_{\text{A}}\boldsymbol{\gamma}_{\text{A}}^{\text{H}} \tag{39}$$

where $\mathbf{I}_N$ is an $N \times N$ identity matrix.

Fig. 10 plots the magnitude of the covariance matrix of an example $\boldsymbol{\gamma}_{\text{A}}$ coming from our experimental data set for two extreme cases of ϕ. Here, it is interesting to see that when $\phi = 1/N$, the second term in (39) vanishes and, hence, the covariance matrix of the transmit sequence will be identity. The significance of this finding is that when $\phi = 1/N$, the signal direction $\boldsymbol{\gamma}_{\text{A}}$ will not be observable in the covariance matrix $[\mathbf{x}_k \mathbf{x}_k^{\text{H}}]$ and, thus, any method that seeks to estimate $\boldsymbol{\gamma}_{\text{A}}$ by exploring the second order moments of $\mathbf{x}_k$ will be unsuccessful. Next, we use numerical results to evaluate the effectiveness of the blind attack from a sophisticated adversary as discussed in Section V-B. The goal of this simulation is to examine the number of symbols K that can be sent with a given key $\boldsymbol{\gamma}_{\text{A}}$. To start, Alice transmits K symbols with a given spreading code sequence obtained from the experimental data set. The information symbols are encoded with binary phase-shift keying (BPSK) so that $s_k = \pm\, \sigma_s$ and we assume the worst-case eavesdropper who has zero channel noise, and thus $\mathbf{z}_k = \mathbf{x}_k$.

Once Eve receives K symbols, she constructs the matrix $\mathbf{Z}$ as in (34). Next, the Rayleigh-Ritz theorem (36) is applied to obtain a blind estimate of the spreading code sequence. This process is run for increasing values of K from 4 to 256, and different choices of ϕ. To evaluate the effectiveness of this attack, we calculate the similarity between $\hat{\boldsymbol{\gamma}}_A$ and $\boldsymbol{\gamma}_{\text{A}}$ using (29).

Fig. 11 plots the 99th percentile of ρ_{AE}, when $\boldsymbol{\gamma}_{\text{E}}$ is set equal to $\hat{\boldsymbol{\gamma}}_A$, as a function of K for varying values of ϕ. The 99th percentile shows the line where 99% of the time, ρ_{AE} remains below it. As observed for larger values of ϕ, i.e., when the level of artificial noise is relatively low, the eavesdropper may be able to obtain a reasonable estimate of $\boldsymbol{\gamma}_{\text{A}}$ within a relatively small number of observed samples. However, as ϕ increases, it becomes more difficult to estimate $\boldsymbol{\gamma}_{\text{A}}$.

For the golden ratio of $\phi = 1/N$, since $[\mathbf{x}_k \mathbf{x}_k^{\mathrm{H}}]$ become the identity matrix, almost all the estimates of $\boldsymbol{\gamma}_{\mathrm{A}}$ remain nearly orthogonal to $\boldsymbol{\gamma}_{\mathrm{A}}$, hence, an almost sure secure communication can be guaranteed.

VII. Conclusion

In this paper, we proposed and studied a secret-key enabled secure information transmission system for spread-spectrum communication. We presented a method where two asynchronous radios can exchange a set of spreading codes through the use of the reciprocal wireless channel. The key itself is shown to have been made stronger through the use of a method that we named SPC (Strongest Path Cancellation). We validated our approach through both simulation and experimentation and showed that the use of SPC greatly aids our proposed secure information transmission solution.

The secure information transmission system proposed here introduces the concept of artificial noise to multi-carrier spread-spectrum systems as a means of enhancing the physical-layer security in wide band communications. The solution was tested against both a passive eavesdropper who follows the same procedure of Alice and Bob as well as the more sophisticated adversary who seeks to blindly determine the key used by Alice. In the first situation, it was shown that, despite SPC introducing a slight decorrelation between keys of Alice and Bob, the probability of a secrecy outage remains in favor of the key generated using SPC. For the more sophisticated adversary, we make the following observation. When Alice and Bob have enough SNR to take advantage of, by adding sufficient artificial noise they will be able to communicate many information symbols securely.

Appendix

Derivation of SNR After despreading

Using (26), we note that Bob's received signal after despreading is

$$\boldsymbol{\gamma}_{\mathrm{B}}^{\mathrm{H}} \mathbf{y}_k = \boldsymbol{\gamma}_{\mathrm{B}}^{\mathrm{H}} \boldsymbol{\gamma}_{\mathrm{A}} s_k + \boldsymbol{\gamma}_{\mathrm{B}}^{\mathrm{H}} \mathbf{v}_k + \boldsymbol{\gamma}_{\mathrm{B}}^{\mathrm{H}} \boldsymbol{\eta}_k. \tag{40}$$

The SNR after despreading is taken to be

$$\mathrm{SNR}_{\mathrm{B}}^{\mathrm{o}} = \frac{\mathrm{Var}[\boldsymbol{\gamma}_{\mathrm{B}}^{\mathrm{H}} \boldsymbol{\gamma}_{\mathrm{A}} s_k]}{\mathrm{Var}[\boldsymbol{\gamma}_{\mathrm{B}}^{\mathrm{H}} \mathbf{v}_k + \boldsymbol{\gamma}_{\mathrm{B}}^{\mathrm{H}} \boldsymbol{\eta}_k]}. \tag{41}$$

The numerator in (41) is evaluated as

$$\mathrm{Var}[\boldsymbol{\gamma}_{\mathrm{A}}^{\mathrm{H}} \boldsymbol{\gamma}_{\mathrm{B}} s_k] = \rho_{\mathrm{AB}} \sigma_s^2. \tag{42}$$

For the denominator, we know that the noise and artificial noise are uncorrelated and consequently the variance of the two terms can be separated. Using (17), we get

$$\begin{aligned} \mathrm{Var}[\boldsymbol{\gamma}_{\mathrm{B}}^{\mathrm{H}} \mathbf{v}_k] &= \left[\left| \boldsymbol{\gamma}_{\mathrm{B}}^{\mathrm{H}} \mathbf{v}_k \right|^2 \right] \\ &= \sigma_w^2 (1 - \rho_{\mathrm{AB}}). \end{aligned} \tag{43}$$

and since $\boldsymbol{\gamma}_{\mathrm{B}}$ and $\boldsymbol{\eta}_k$ are uncorrelated, one will find that

$$\mathrm{Var}(\boldsymbol{\gamma}_{\mathrm{B}}^{\mathrm{H}} \boldsymbol{\eta}_k) = \frac{\sigma_\eta^2}{N} \tag{44}$$

where $\sigma_\eta^2 = [\boldsymbol{\eta}_k^{\mathrm{H}} \boldsymbol{\eta}_k]$ is the total noise power across the occupied bandwidth. Finally, by combining (42), (43), and (44), and recalling (24) and (29), one can obtain (28).

Acknowledgment

The United States Government retains and the publisher, by accepting the article for publication, acknowledges that the United States Government retains a nonexclusive, paid-up, irrevocable, world-wide license to publish, or reproduce the published form of this work, or allow others to do so, for United States Government purposes. STI Number: INL/JOU-16-40352.

References

[1] K. Cheun, K. Choi, H. Lim, and K. Lee, "Antijamming performance of a multicarrier direct-sequence spread-spectrum system," *IEEE Trans. Commun.*, vol. 47, no. 12, pp. 1781–1784, Dec. 1999.

[2] Y.-S. Shiu, S. Y. Chang, H.-C. Wu, S. C.-H. Huang, and H.-H. Chen, "Physical layer security in wireless networks: A tutorial," *IEEE Wireless Commun.*, vol. 18, no. 2, pp. 66–74, Apr. 2011.

[3] T. Kang, X. Li, C. Yu, and J. Kim, "A survey of security mechanisms with direct sequence spread spectrum signals," *J. Comput. Sci. Eng.*, vol. 7, no. 3, pp. 187–197, 2013.

[4] M. A. Abu-Rgheff, *Introduction to CDMA Wireless Communications*. San Francisco, CA, USA: Academic, 2007.

[5] T. Li, J. Ren, Q. Ling, and A. Jain, "Physical layer built-in security analysis and enhancement of CDMA systems," in *Proc. IEEE Military Commun. Conf. (MILCOM)*, vol. 2. Oct. 2005, pp. 956–962.

[6] H. Imai, *Wireless Communications Security*. Norwood, MA, USA: Artech House, 2005.

[7] W. Diffie and M. E. Hellman, "New directions in cryptography," *IEEE Trans. Inf. Theory*, vol. IT-22, no. 6, pp. 644–654, Nov. 1976.

[8] J. Zhang, T. Q. Duong, A. Marshall, and R. Woods, "Key generation from wireless channels: A review," *IEEE Access*, vol. 4, pp. 614–626, 2016.

[9] K. Ren, H. Su, and Q. Wang, "Secret key generation exploiting channel characteristics in wireless communications," *IEEE Wireless Commun.*, vol. 18, no. 4, pp. 6–12, Aug. 2011.

[10] Y. E. H. Shehadeh and D. Hogrefe, "A survey on secret key generation mechanisms on the physical layer in wireless networks," *Secur. Commun. Netw.*, vol. 8, no. 2, pp. 332–341, 2015.

[11] Y. Zou, J. Zhu, X. Wang, and L. Hanzo, "A survey on wireless security: Technical challenges, recent advances, and future trends," *Proc. IEEE*, vol. 104, no. 9, pp. 1727–1765, Sep. 2016.

[12] B. He, X. Zhou, and T. D. Abhayapala, "Wireless physical layer security with imperfect channel state information: A survey," *ZTE Commun.*, vol. 11, no. 2, pp. 11–19, 2013.

[13] M. Bloch, J. Barros, M. R. D. Rodrigues, and S. W. McLaughlin, "Wireless information-theoretic security," *IEEE Trans. Inf. Theory*, vol. 54, no. 6, pp. 2515–2534, Jun. 2008.

[14] H. Koorapaty, A. A. Hassan, and S. Chennakeshu, "Secure information transmission for mobile radio," *IEEE Commun. Lett.*, vol. 4, no. 2, pp. 52–55, Feb. 2000.

[15] A. O. Hero, "Secure space-time communication," *IEEE Trans. Inf. Theory*, vol. 49, no. 12, pp. 3235–3249, Dec. 2003.

[16] G. R. Tsouri and D. Wulich, "Reverse piloting protocol for securing time varying wireless channels," in *Proc. Wireless Telecommun. Symp*, Apr. 2008, pp. 125–131.

[17] S. Goel and R. Negi, "Guaranteeing secrecy using artificial noise," *IEEE Trans. Wireless Commun.*, vol. 7, no. 6, pp. 2180–2189, Jun. 2008.

[18] A. L. Swindlehurst, "Fixed SINR solutions for the MIMO wiretap channel," in *Proc. IEEE Int. Conf. Acoust., Speech Signal Process. (ICASSP)*, Apr. 2009, pp. 2437–2440.

[19] X. Zhou and M. R. McKay, "Secure transmission with artificial noise over fading channels: Achievable rate and optimal power allocation," *IEEE Trans. Veh. Technol.*, vol. 59, no. 8, pp. 3831–3842, Oct. 2010.

[20] T. S. Rappaport *et al.*, *Wireless Communications: Principles and Practice*. Englewood Cliffs, NJ, USA: Prentice-Hall, 2001.

[21] B. Farhang-Boroujeny, *Signal Processing Techniques for Software Radios*. Morrisville, NC, USA: Lulu Publishing, 2008.

[22] R. Frank, S. Zadoff, and R. Heimiller, "Phase shift pulse codes with good periodic correlation properties (Corresp.)," *IRE Trans. Inf. Theory*, vol. 8, no. 6, pp. 381–382, Oct. 1962.
[23] D. Chu, "Polyphase codes with good periodic correlation properties (Corresp.)," *IEEE Trans. Inf. Theory*, vol. IT-18, no. 4, pp. 531–532, Jul. 1972.
[24] S. Sesia, M. Baker, and I. Toufik, *LTE—The UMTS Long Term Evolution: From Theory to Practice*. New York, NY, USA: Wiley, 2011.
[25] A. Majid, H. Moradi, and B. Farhang-Boroujeny, "Secure information transmission in filter bank multi-carrier spread spectrum systems," in *Proc. IEEE Military Commun. Conf. (MILCOM)*, Oct. 2015, pp. 287–293.
[26] D. L. Wasden, H. Moradi, and B. Farhang-Boroujeny, "Design and implementation of an underlay control channel for cognitive radios," *IEEE J. Sel. Areas Commun.*, vol. 30, no. 10, pp. 1875–1889, Nov. 2012.
[27] J. Barros and M. R. D. Rodrigues, "Secrecy capacity of wireless channels," in *Proc. IEEE Int. Symp. Inf. Theory*, Jul. 2006, pp. 356–360.
[28] X. Zhou, M. R. McKay, B. Maham, and A. Hjørungnes, "Rethinking the secrecy outage formulation: A secure transmission design perspective," *IEEE Commun. Lett.*, vol. 15, no. 3, pp. 302–304, Mar. 2011.
[29] F. Zhang, *Matrix Theory: Basic Results and Techniques*. New York, NY, USA: Springer, 2011.
[30] T. Haddadin *et al.*, "An underlay communication channel for 5G cognitive mesh networks: Packet design, implementation, analysis, and experimental results," in *Proc. IEEE Int. Conf. Commun. Workshops (ICC)*, May 2016, pp. 498–504.
[31] A. Majid, "Secure communications in filter-bank multi-carrier spread spectrum systems," Ph.D. dissertation, Dept. Elect. Comput. Eng., Univ. Utah, Salt Lake City, UT, USA, 2017.

Arslan Javaid Majid received the B.S. and M.S. degrees and the Ph.D. degree, under the supervision of Dr. B. Farhang-Boroujeny, from The University of Utah, in 2012 and 2017, respectively, all in electrical and computer engineering. He is currently a Wireless Researcher with the Idaho National Laboratory, Idaho Falls, ID, USA. His research interests include signal processing, multicarrier wireless communications, spread-spectrum communications, physical-layer security, and software-defined radio implementations.

Hussein Moradi received the bachelor's degree from The University of Texas at Arlington, TX, USA, and the master's and Ph.D. degrees from Southern Methodist University, Dallas, TX. He held director positions for wireless research and development with Kyocera Wireless, VeriFone Inc., and NEC America, advancing state-of-the-art wireless devices. In 2009, he joined the Idaho National Laboratory as a Chief Wireless Scientist for National and Homeland Security. He brings over 30 years of experience in corporate research and leadership development. As a recognized national thought leader in telecommunications, he holds five international patents in spectrum sharing and three pending in wireless communications systems shaping the next generation wireless global standardization. He has developed GSM/GPRS/EDGE, CDMA/EVDO, 802.11, BT 2.5G/3G VoIP wireless handsets and has domain expertise in WiMAX, LTE, and physical-layer spectrum agile communication technologies. His research interests include systems engineering, RF layer, ASIC, hardware and embedded software development for computing and wireless telecommunications devices. He received the 2012 Research and Development 100 Award for his wireless spectrum communication system innovation.

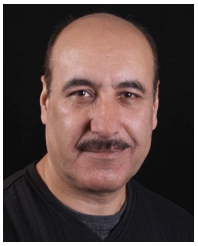

Behrouz Farhang-Boroujeny (M'84–SM'90) received the B.Sc. degree in electrical engineering from Tehran University, Iran, in 1976, the M.Eng. degree from the University of Wales Institute of Science and Technology, U.K., in 1977, and the Ph.D. degree from the Imperial College, University of London, U.K., in 1981. From 1981 to 1989, he was with the Isfahan University of Technology, Isfahan, Iran. From 1989 to 2000, he was with the National University of Singapore. Since 2000, he has been with The University of Utah. He is an expert in the general area of signal processing. His current scientific interests include adaptive filters, multicarrier communications, detection techniques for space-time coded systems, and cognitive radio. He has made significant contributions to the areas of adaptive filters theory, acoustic echo cancellation, magnetic/optical recoding, and digital subscriber line technologies. He is the author of the books *Adaptive Filters: Theory and Applications* (John Wiley & Sons, 1998 and 2013) and *Signal Processing Techniques for Software Radios*, (Lulu Publishing, 2009 and 2010) (second edition). He received the UNESCO Regional Office of Science and Technology for South and Central Asia Young Scientists Award in 1987. He served as an Associate Editor of the IEEE TRANSACTIONS ON SIGNAL PROCESSING from 2002 to 2005, and the IEEE SIGNAL PROCESSING LETTERS from 2008 to 2010. He has also been involved in various IEEE activities, including the chairmanship of the Signal Processing/Communications chapter of the IEEE of Utah in 2004 and 2005.